

---

# Can Backdoor Attacks Survive Time-Varying Models?

---

**Huiying Li**  
Computer Science  
University of Chicago  
huiyingli@cs.uchicago.edu

**Arjun Nitin Bhagoji**  
Computer Science  
University of Chicago  
abhagoji@cs.uchicago.edu

**Ben Y. Zhao**  
Computer Science  
University of Chicago  
ravenben@cs.uchicago.edu

**Haitao Zheng**  
Computer Science  
University of Chicago  
htzheng@cs.uchicago.edu

## Abstract

Backdoors are powerful attacks against deep neural networks (DNNs). By poisoning training data, attackers can inject hidden rules (backdoors) into DNNs, which only activate on inputs containing attack-specific triggers. While existing work has studied backdoor attacks on a variety of DNN models, they only consider *static* models, which remain unchanged after initial deployment.

In this paper, we study the impact of backdoor attacks on a more realistic scenario of time-varying DNN models, where model weights are updated periodically to handle drifts in data distribution over time. Specifically, we empirically quantify the “survivability” of a backdoor against model updates, and examine how attack parameters, data drift behaviors, and model update strategies affect backdoor survivability. Our results show that one-shot backdoor attacks (i.e., only poisoning training data once) do not survive past a few model updates, even when attackers aggressively increase trigger size and poison ratio. To stay unaffected by model update, attackers must continuously introduce corrupted data into the training pipeline. Together, these results indicate that when models are updated to learn new data, they also “forget” backdoors as hidden, malicious features. The larger the distribution shift between old and new training data, the faster backdoors are forgotten. Leveraging these insights, we apply a smart learning rate scheduler to further accelerate backdoor forgetting during model updates, which prevents one-shot backdoors from surviving past a single model update.

## 1 Introduction

Given their dependence on large volumes of training data [28, 31], deep neural networks (DNNs) are particularly vulnerable to data poisoning attacks. In a backdoor attack, attackers corrupt training data in order to produce misclassifications on inputs with specific characteristics [4, 8, 25]. Existing work has shown that backdoors are easy to inject and hard to detect, and are considered the most worrisome attacks in a recent industry survey [18]. A number of proposed defenses detect and mitigate backdoor attacks [7, 23, 24, 37, 39], but have generally fallen short when evaluated in a variety of attack settings, including transfer learning [44], federated learning [1, 40, 43] and physical attack scenarios [22, 41].

A major shortcoming of current work on backdoor attacks is a common assumption that models are *static* and do not change over time. In reality, most production ML models are continuously

updated, either to incorporate more labeled data, or to adapt to evolving changes in the targeted data distribution [17, 26]. For example, ML models in recommendation systems, user behavior classification, even road recognition in self-driving vehicles, all need to deal with underlying target distributions that shift over time [47]. If a deployed model’s target data distribution evolves, but the model does not, the mismatch will produce significant drops in performance.

We use **time-varying models** to refer to models that are continuously updated with new training data. There are multiple ways of updating time-varying models, including online learning, batch/(mini)batch incremental learning, and offline learning [10, 11, 30, 32, 46]. Among those, offline learning provides more stable model performance compared to other alternatives, since model owners can train models until they achieve specific properties, e.g. reaching specific targets for accuracy. More specifically, models can be retrained from scratch, or fine-tuned. Training a modern DNN model from scratch takes significant data and computational resources, while fine-tuning a pretrained model can be significantly more efficient and less costly [34, 36, 48]. Thus our work focuses on time-varying models updated via fine-tuning.

Under a static view of models targeted by backdoor attacks, once a model is poisoned, it is and remains vulnerable to attack. However, time-varying models undergoing periodic fine-tuning are **dynamic**, and the fine-tuning process has significant implications on backdoor attacks.

**Our Contributions.** In this paper, we take an empirical approach to studying backdoor attacks on time-varying models, which are fine-tuned continuously with new data. We show that this dynamic context has significant implications on traditional backdoor attacks. Attacks conducted using a fixed amount of poison events will only be effective during a “window of vulnerability,” before the embedded backdoor is “forgotten” and its triggers ineffective. Faster/bigger shifts in the underlying (benign) data distribution will also accelerate the backdoor forgetting process and shorten the window of vulnerability. In this paper, we empirically measure the window of vulnerability caused by a backdoor attack on time-varying models, defined as the **backdoor survivability**. We perform extensive experiments to understand the impact of different attack configurations, data drift behaviors, and training strategies in this time-varying domain, and show that well-chosen training strategies can significantly reduce the efficacy of backdoor attacks soon after the infusion of poison data, thus lowering their survivability against model updates.

## 2 Background and Definitions

In this section, we provide the necessary background and formal definitions on backdoor attacks and time-varying DNN models. Our discussion and definitions focus on image-based classification tasks.

### 2.1 Backdoor Attacks

Backdoors are the most common and effective form of data poisoning attacks, and also the most concerning type of attacks against machine learning systems according to a recent industry survey [18]. In a backdoor attack, an attacker injects hidden behaviors into a model by controlling and modifying a (small) fraction of its training data, i.e., adding a trigger (usually a small perturbation) to normal images and labeling them with a desired target label. This forces the trained model to associate the trigger’s presence with the target label. At test time, any input containing the trigger will be (mis)classified as the target label. Note this only requires corrupting a small fraction (e.g., 5-10%) of the training data, without any access to the training process [4, 8].

One can formally define a backdoor attack by its trigger  $(mask, \delta)$ , target label  $y_t$ , and poison rate  $(\alpha)$ , where  $mask$  is a matrix specifying the size, shape, and location of the trigger,  $\delta$  defines the trigger pixel values, and  $\alpha$  defines the fraction of training data modified by the attacker. A normal training sample  $x$ , after modified by the attacker, becomes a poisoned input  $A(x, mask, \delta)$  with label  $y_t$ :

$$A(x, mask, \delta) = (1 - mask) \circ x + mask \circ \delta \tag{1}$$

where  $\circ$  denotes the matrix element-wise product. By providing a collection of poisoned training data  $(X_a)$ , the attacker is able to inject trigger-specific classification rules into the trained model, i.e.,

$$\min_{\theta, x \in X_a} \ell(y_t, F_{\theta}(A(x, mask, \delta))) \tag{2}$$

Besides highly effective, backdoor attacks are also stealthy and hard to detect. Unlike traditional poisoning attacks that degrade a model’s classification accuracy on normal inputs [2, 42, 33], backdoor attacks typically do not affect normal classification accuracy, and only cause misclassification on inputs containing attack-specific triggers. While significant efforts were spent on detecting and/or removing backdoors on DNN models (e.g., [7, 37, 23, 39, 24, 29]), they all face limitations [6, 38]. Recent efforts have also produced a rich set of attack variants (e.g., [44, 43, 1, 40, 22, 27, 41, 21]) that display stronger stealthiness and effectiveness. In particular, physical backdoor attacks [41], by using everyday objects as triggers, break all tested SOTA backdoor defenses.

Finally, we note that existing works on backdoor attacks have all taken a “static” view, i.e. they target static models that remain unchanged once deployed. In this case, a successfully injected backdoor is always present in the model.

## 2.2 Time-Varying Models

Machine learning models are trained based on the assumption that the distribution of test data is similar to that of training data. In reality, this is often not true. Drifts in data distribution, if not addressed, can significantly affect model accuracy. Therefore, it is a common practice to update a deployed model over time in order to handle drifts in data distribution [3, 34, 17, 26]. As such, a model in production is rarely if ever static – its model weights change over time. We refer to these models as time-varying models, and formally define them below:

**Definition 1** (Time-varying models). *A time-varying model  $F$ , observed between 0 and  $t$ , is a sequence of models  $\{F_i\}_{i=0}^t$  trained from sequentially available data  $\{D_i\}_{i=0}^t$  such that after the  $i^{\text{th}}$  update, the model  $F_i = \mathbf{g}(\{D_k\}_{k \leq i}, \{F_k\}_{k < i})$ . Here  $\mathbf{g}(\cdot)$  is any training function. The new training data available at the  $i^{\text{th}}$  update ( $D_i$ ) is drawn from a distribution  $\mathcal{D}_i$ .*

**Model Update Strategies.** The update strategy can be broadly categorized into three groups: 1) training from scratch using all training data (original + new), 2) training from scratch using new training data, and 3) fine-tuning the current model with new training data.

1) *Training from scratch using all training data*, i.e.,  $F_t = \mathbf{g}(\cup_{i \leq t} D_i, \emptyset)$ : Model owners can continuously integrate new data into the training set, and retrain a new version of the model from scratch using the combined training set. Here, training overhead increases over time while the influence of new training data  $D_t$  is limited, potentially impeding the model’s ability to learn the new data distribution.

2) *Training from scratch using new training data*, i.e.,  $F_t = \mathbf{g}(D_t, \emptyset)$ : If the production data varies significantly over time, there is little incentive to train the model using “outdated” data, but to train a completely new model using just the new data  $D_t$ . However, this strategy places significant size and diversity requirements on training data collection, which could either slow down model updates or degrade model accuracy (due to overfitting).

3) *Fine-tuning the current model with new training data*, i.e.,  $F_t = \mathbf{g}(D_t, F_{t-1})$ : Training high-performance production models usually takes enormous amounts of both computational resources and labeled training data, making it infeasible to update a model by training from scratch. Many ML practitioners choose to fine-tune the current model  $F_{t-1}$  using the new data  $D_t$ , which allows the updated model  $F_t$  to learn the new data distribution efficiently.

We note that model updates can also come from certain learning paradigms such as online learning, batch/mini-batch incremental learning, and offline continuous learning like transfer learning [30, 11, 32, 46, 10, 36, 48]. Online learning operates on a per sample basis ( $|D_i| = 1, \forall i$ ) while batch/(mini) batch incremental learning assumes  $|D_i| = c, \forall i$ , where  $c$  is the batch size.

**Data Distribution Drifts.** It is clear that the behavior of time-varying models depends on how data distribution drifts over time. In this paper, we assume the model owner monitors the model accuracy and triggers a model update upon detecting a given level of distribution drift (also suggested by [3]). This creates an “even” distribution drift between consecutive model updates.

**Definition 2** (Even data distribution shifts). *A time-varying model  $F$  is a classification function that projects an input  $x \in \mathbb{R}^d$  to an output probability distribution on labels  $y \in \mathbb{R}^N$ . At the  $i$ th model update, the new training data  $D_i$  reflects the joint distribution over input  $x$  and label  $y$  ( $x \in \mathbb{R}^d \times y \in \mathbb{R}^N$ ):  $P_i$ . Between model updates, the data distribution shift is even if*

$$\rho(P_i, P_{i+1}) = p, \quad \forall i, \quad (3)$$

where  $\rho(P, Q)$  is some distance function between distributions  $P$  and  $Q$ , and  $p$  is the “step” of the distribution shift.

### 3 Backdoor Survivability against Model Updates

In this paper, we study the impact of backdoor attacks on a more realistic context of time-varying DNN models that are updated over time to handle data distribution shifts. To the best of our knowledge, this is the first study on backdoor attacks against time-varying models.

We formulate our study to empirically examine the “survivability” of a successfully injected backdoor against subsequent model updates, and how backdoor survivability is affected by different attack configurations, data drift behaviors, and model update strategies. We believe these results offer a more in-depth understanding on the impact of backdoor attacks on production models, in terms of both attack overhead and damage on the models. We build on them to develop model training/updating strategies that further reduce backdoor survivability (§6).

In the following, we first introduce the underlying threat model, and then describe the setup of our empirical study, followed by a formal definition of backdoor survivability and some initial observations. We present the detailed results later in §4 – §5.

#### 3.1 Threat Model

Like existing works on backdoor attacks, we assume that the attacker is able to control or modify a fraction of the model training data, but has no knowledge of the model architecture, weights, or training hyperparameters during initial model training and subsequent model updates. Also, the attacker cannot predict the training data distribution  $\{P_i\}_{i=0}^t$ .

We consider two types of attacks based on how “persistent” the poisoning is carried out over time:

- **One-shot poisoning:** The attacker is only able to poison the training data once. Without loss of generality, we consider two cases: (i) the attacker poisons  $D_0$  and injects a backdoor into  $F_0$ , the initial model prior to deployments; and (ii) the attacker poisons the data used by a model update  $D_i$  and thus injects a backdoor into  $F_i$  (via fine-tuning). For simplicity, we consider  $i = 1$ .
- **Persistent poisoning:** A more powerful attacker can continuously poison the training data used by subsequent model updates ( $\{D_i\}_{i>0}$ ), e.g., by being a key supplier of the labeled training data.

Given our goal of quantifying backdoor survivability against model updates, we do not consider existing backdoor defenses in this study. Instead, we seek to understand whether and how model updates affect backdoor effectiveness, and whether such natural model variations can be leveraged to build stronger defenses against backdoor attacks.

#### 3.2 Our Empirical Study

We now describe the configuration of our empirical study to examine backdoor survivability.

**Datasets.** We consider two image classification datasets: MNIST [20] and CIFAR10 [16]. For each task, we randomly split its training data into two halves. The first half is assigned as  $D_0$  and used to train the initial model  $F_0$ . The second half and the test data are used to emulate a dynamic data environment, where both the training and test data distributions vary over time.

In this work, we produce parameterized data dynamics by applying image transformations progressively (i.e., rotation, changing brightness, hue and saturation), similar to the method used by [17] to study gradual domain adaptation. These transformations also reflect practical scenarios where a deployed camera adjusts its view angle over time, or when the camera’s view is shadowed by a new structure nearby, or when the camera’s color spectrum varies due to hardware aging or dust accumulation.

In our experiments, the default data drift  $p$  between any two consecutive updates is caused by rotating the current images by  $2^\circ$ . These drifts, if not addressed, cause significant degradation to model performance (e.g., the classification accuracy drops from 92% to 47% after 14 rounds of  $2^\circ$  rotation). More details on other distribution drifts are listed in Appendix.

**DNN Models and Updates.** We consider three model architectures: ResNet-9 [14], ResNet18 [9] and DenseNet121 [13]. We find that they produce the same trends on backdoor behaviors on both

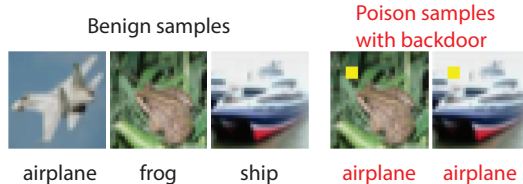


Figure 1: Examples of benign and poisoned training data (and their labels), using a  $4 \times 4$  yellow square as the default backdoor trigger.

static models ( $F_0$ ) and time-varying models ( $F_t$ ). For brevity, we only present the results for ResNet-9 [14], which is optimized for fast training. For both CIFAR10 and MNIST, we train the initial model  $F_0$  to reach a high normal classification accuracy: 92% for CIFAR10 and 98% for MNIST.

We consider fine-tuning as the default model update strategy due to its efficiency and practicality (as discussed in §2.2). At the  $i^{th}$  update, we fine-tune model  $F_{i-1}$  using new training data  $D_i$  to produce  $F_i$ , by applying stochastic gradient descent (SGD) optimizers with weight decay and momentum. We set the default learning rate to 0.01, and the default fine-tuning epochs to 5. Additional details of model training and updating are listed in Appendix.

**Attack Configuration.** By default, the attacker is able to poison 5% of the training data  $D_i$ , using a  $4 \times 4$  yellow square as the trigger. Figure 1 lists a few examples from CIFAR10. We conduct detailed experiments to explore the impact of poison ratio, trigger size, location, and shape in §4. For all our experiments, we ensure that the backdoor, when injected into the current operating model, is effective, i.e., its attack success rate is at least 95% without affecting the model’s normal accuracy.

For each experiment, we first randomly generate five trained  $F_0$  instances. Then for each instance, we run 14 additional model updates upon a given level of data shift  $p$  if the attacker chooses to poison  $D_0$ , and 15 additional model updates if the attacker chooses to poison  $D_1$ . We report the classification results as the average and std of the 5 instances. We run all the experiments using the FFCV library [19] on an NVIDIA TITAN RTX GPU with 24,576MB GPU memory.

### 3.3 Defining Backdoor Survivability

We define the survivability of a backdoor as the “window of vulnerability” it produces on the target time-varying model:

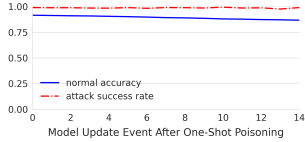
**Definition 3** ( $\gamma$ -survivability of a backdoor attack). *The  $\gamma$ -survivability of a backdoor is the maximum number of subsequent model updates following its initial injection, during which the attack success rate on the target model remains above a threshold  $\gamma$ .*

Here  $\gamma$  can vary depending on the definition of “model vulnerability.” Since the choice of  $\gamma$  may vary based on context and application, we consider three values in our study: 0.25, 0.5 and 0.75. Since our experiments run up to 14 subsequent model updates after a backdoor is injected, if the attack success rate remains above  $\gamma$  after these updates, its  $\gamma$ -survivability = 14.

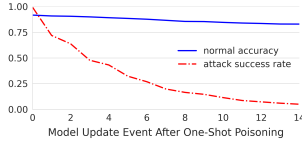
**Initial Observations.** For one-shot poisoning attacks, our initial hypothesis is that the attack success rate should always decrease over time, because as more benign samples are used to train the model, the influence of the poisoned samples should reduce. However, the actual result is much more dependent on the model update strategy than the accumulated poison ratio. Figure 2(a) shows the backdoor remains 100% successful when the model is retrained from scratch using all data, because poison data remains in the training set. But when the model is fine-tuned to learn new (benign) data, the backdoor gradually degrades (Figure 2 (b)). Model update strategy clearly plays a significant role in backdoor survivability. It also motivates us to **focus on fine-tuning based model updates** in our subsequent experiments.

## 4 Impact of Attack Strategies and Configurations

We now present the results of  $\gamma$ -survivability under different attack strategies and configurations. We consider both *one-shot poisoning*, where the attacker has one chance to poison the training data, and *persistent poisoning* where the attacker can continuously supply poisoned data samples.



(a) Full training using all data



(b) Fine-tuning with new data

Figure 2: Normal accuracy and backdoor attack success rate for time-varying models using different model update strategies. We consider one-shot poisoning attacks that poison training data  $D_1$  to inject backdoors.

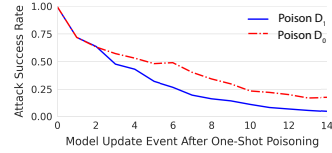


Figure 3: Backdoor attack success rates when using one-shot poisoning of  $D_0$  or  $D_1$  to inject backdoors.

Metrics	poison ratio					trigger size		
	0.01	0.02	0.05	0.1	0.2	$4 \times 4$	$8 \times 8$	$16 \times 16$
$\gamma = 0.25$	$12.20 \pm 1.94$	$10.40 \pm 2.58$	$9.60 \pm 3.07$	$7.40 \pm 3.01$	$5.40 \pm 5.08$	$9.60 \pm 3.07$	$11.60 \pm 1.85$	$14.00 \pm 0.00$
$\gamma = 0.5$	$7.40 \pm 1.02$	$6.60 \pm 2.42$	$4.80 \pm 2.04$	$3.00 \pm 3.16$	$1.60 \pm 1.85$	$4.80 \pm 2.04$	$9.80 \pm 2.40$	$13.60 \pm 0.49$
$\gamma = 0.75$	$2.80 \pm 1.47$	$2.20 \pm 1.47$	$0.80 \pm 0.75$	$0.60 \pm 0.80$	$0.00 \pm 0.00$	$0.80 \pm 0.75$	$4.20 \pm 3.49$	$11.80 \pm 1.72$

(a) poisoning  $D_0$ 

Metrics	poison ratio					trigger size		
	0.01	0.02	0.05	0.1	0.2	$4 \times 4$	$8 \times 8$	$16 \times 16$
$\gamma = 0.25$	$4.40 \pm 1.20$	$4.80 \pm 1.17$	$5.40 \pm 0.80$	$5.80 \pm 1.33$	$7.40 \pm 1.20$	$5.40 \pm 0.80$	$7.80 \pm 1.72$	$13.80 \pm 0.40$
$\gamma = 0.5$	$1.80 \pm 1.17$	$1.60 \pm 0.49$	$2.40 \pm 0.49$	$2.80 \pm 0.40$	$3.40 \pm 1.02$	$2.40 \pm 0.49$	$5.00 \pm 1.10$	$12.20 \pm 1.33$
$\gamma = 0.75$	$0.00 \pm 0.00$	$0.00 \pm 0.00$	$0.20 \pm 0.40$	$0.20 \pm 0.40$	$0.20 \pm 0.40$	$0.20 \pm 0.40$	$1.60 \pm 0.49$	$9.60 \pm 2.24$

(b) poisoning  $D_1$ 

Table 1: Backdoor  $\gamma$ -survivability using two types of one-shot poisoning: (a) poisoning  $D_0$  to inject backdoors into  $F_0$  via full training and (b) poisoning  $D_1$  to inject backdoors into  $F_1$  via fine-tuning.

#### 4.1 One-shot Poisoning

As discussed in §3.1, we consider two attack scenarios based on how backdoors are injected into the target model. The attacker can (i) poison  $D_0$  to inject a backdoor to the original model  $F_0$  via training from scratch (or full training); or (ii) poison  $D_1$  to inject a backdoor to  $F_1$  via fine-tuning. While both can inject backdoors successfully, we want to understand how injection methods affect the backdoors’ survivability against model updates. We are also interested in if/how backdoor survivability is affected by attacker-side parameters, including poison ratio, trigger size, location and shape.

We show key results for CIFAR10. Results for MNIST are highly consistent and included in Appendix. Figure 3 compares the attack success rate over time when poisoning  $D_0$  or  $D_1$ . Table 1 studies the impact of poison ratio and trigger size. Results on trigger location and shape are also included in Appendix for brevity. We make five key observations from these results.

**Fine-tuning based model updates gradually remove one-shot backdoors.** Figure 3 shows that using either injection method, one-shot backdoor success rate degrades with additional model updates. After a poisoned model learns backdoors as hidden classification features, each updated version gradually forgets these features over time, if model updates are benign and there are no poisoned samples to reinforce the model’s memory. While they were not designed to address backdoors, fine-tuning based model updates *naturally* degrade one-shot backdoors over time.

This finding is similar to those discovered in continual learning, where learned “features” or “examples” tend to be forgotten by neural networks once they become absent in subsequent training data [5, 35]. These existing analyses, however, only considered non-adversarial scenarios like natural data dynamics or domain adaptation. It is interesting that intentionally injected attack features behave similarly, and are gradually “forgotten” by time-varying models. This property can clearly be leveraged to build *natural robustness* against backdoors.

**Backdoors injected via full training survive longer than those injected via fine-tuning.** Another interesting finding is that backdoors embedded in  $F_0$  carry more “strength” and survive longer against model updates compared to those injected into  $F_1$ . For CIFAR10 and 5% poison ratio, the 0.25-survivability is considerably different: 9.6 for  $F_0$  backdoors and 5.4 for  $F_1$  backdoors. This is likely because backdoors injected via full training embed the hidden features more broadly into the model, making them harder to “remove” by subsequent fine-tuning. On the other hand, poisoning  $D_0$

Metrics	$\alpha=0.05$			$\alpha=0.1$		
	$k_p=1$	$k_p=2$	$k_p=5$	$k_p=1$	$k_p=2$	$k_p=5$
$\gamma = 0.25$	5.40/0.008	5.80/0.013	5.80/0.023	5.80/0.015	6.80/0.023	7.20/0.041
$\gamma = 0.5$	2.40/0.015	3.40/0.019	3.20/0.030	2.80/0.026	3.80/0.035	4.00/0.056
$\gamma = 0.75$	0.20/0.042	1.40/0.029	1.00/0.042	0.20/0.083	1.40/0.059	1.20/0.081

Table 2: The optimal estimate of  $k_w$  and the minimum poison overhead  $O$  of clustered and periodic poisoning, under different poison ratio  $\alpha$ . Here each cell entry represents  $k_w/O$ .

Subsequent poison ratio	0.0001	0.0002	0.0005	0.001	0.002	0.005
$\gamma = 0.25$	13.60 $\pm$ 0.49	14.00 $\pm$ 0.00	14.00 $\pm$ 0.00	14.00 $\pm$ 0.00	14.00 $\pm$ 0.00	14.00 $\pm$ 0.00
$\gamma = 0.5$	8.40 $\pm$ 2.73	13.80 $\pm$ 0.40	14.00 $\pm$ 0.00	14.00 $\pm$ 0.00	14.00 $\pm$ 0.00	14.00 $\pm$ 0.00
$\gamma = 0.75$	1.40 $\pm$ 0.80	4.80 $\pm$ 1.17	12.00 $\pm$ 2.28	14.00 $\pm$ 0.00	14.00 $\pm$ 0.00	14.00 $\pm$ 0.00

Table 3: Backdoor  $\gamma$ -survivability of persistent poisoning using different subsequent poison ratios.

is generally more challenging, because there is much more opportunity to apply backdoor defenses and detectors on  $F_0$  before its deployment.

**Larger trigger size help improve backdoor survivability.** Our results show that increasing the trigger size leads to a consistent improvement of backdoor survivability, likely because larger triggers introduce stronger deviations on the model’s decision manifolds. However, using larger triggers often means lower attack stealthiness and more visible perturbations. In this case, physical backdoors using real world objects as triggers might achieve a sweet spot of stealth and survivability [41].

**Higher poison ratio does not always increase backdoor survivability.** Existing works have shown that higher poison ratios embed a backdoor with a higher success rate. Surprisingly, it does not always improve backdoor survivability against model updates. Our results show that the answer depends on how the backdoor is injected into the model. If injected via fine-tuning (i.e., on  $F_1$ ), larger poison ratio helps “strengthen” the backdoor against future model updates. But if injected via full-training (i.e., on  $F_0$ ), larger poison ratio can actually “accelerate” the feature forgetting process. This indicates the possible presence of a more complex relationship between backdoors and feature forgetting, which suggests the need for more in-depth study. We leave this to future work.

**Trigger location and shape have much lower impact on survivability.** We experimented with eight different trigger locations. Triggers near the image center help the backdoor survive longer (details in Appendix). This is unsurprising, since all training/test images in our experiments have a single object in the center, thus the center is the key discriminative region for classification [41]. Finally, we also experimented with five trigger shapes (square, 2 types of rectangles, circle and triangle), but found much lower impact compared to other factors (details in Appendix).

## 4.2 Persistent Poisoning

We now consider powerful attackers who can continuously poison the training data. Clearly, if the attacker can poison a sufficient fraction of  $D_i, \forall i$ , the backdoor will remain intact in the time-varying model (which we validated empirically). Here, a more interesting question is: “what can an intelligent attacker do to reduce poison overhead?” Less poison overhead means stealthier attacks. Below we explore two options: (1) clustered periodic poisoning, i.e., poison  $k_p$  updates, skip  $k_w$  updates and repeat; (2) using a poison ratio smaller than that of the initial poison event.

**Periodic poisoning ( $k_p = 1$ ) is more efficient than clustered periodic poisoning ( $k_p > 1$ ).** Table 2 plots the optimal value of  $k_w$  ( $k_w = \gamma$ -survivability) when we vary  $k_p$ . Given  $k_p, k_w$  and a constant poison ratio  $\alpha$ , the minimum poison overhead  $O = \frac{\alpha \cdot k_p}{k_p + k_w}$ , which is also included in the table. We see that  $k_p = 1$  is generally the most efficient. On the other hand, it also shows that if the attacker wants to maintain a reliable attack success rate (e.g., 0.75), they need to **poison every**  $D_i$ .

**Persistent poisoning can maintain injected backdoors at a lower poison ratio.** We first embed a backdoor into  $F_1$  using an initial poison ratio of  $\alpha = 0.05$ , and in the subsequent poisoning, use a much smaller poison ratio (0.0001 – 0.005). Results in Table 3 show that the subsequent poison ratio can be as low as 0.0005 (i.e., 1% of the original  $\alpha$ ) to maintain the injected backdoor.

Shift Step	0	2	4	6
$\gamma = 0.25$	$9.40 \pm 3.07$	$5.40 \pm 0.80$	$4.00 \pm 0.63$	$3.40 \pm 0.80$
$\gamma = 0.5$	$3.40 \pm 1.50$	$2.40 \pm 0.49$	$2.20 \pm 0.75$	$1.80 \pm 0.40$
$\gamma = 0.75$	$0.80 \pm 0.75$	$0.20 \pm 0.40$	$0.40 \pm 0.49$	$0.60 \pm 0.49$

(a) *Rotation*

Shift Step	0	0.02	0.04	0.06
$\gamma = 0.25$	$10.20 \pm 2.79$	$7.00 \pm 1.41$	$4.60 \pm 0.49$	$5.40 \pm 1.02$
$\gamma = 0.5$	$3.60 \pm 1.36$	$3.00 \pm 0.89$	$2.00 \pm 0.63$	$4.00 \pm 0.89$
$\gamma = 0.75$	$0.40 \pm 0.49$	$0.60 \pm 0.49$	$0.00 \pm 0.00$	$0.60 \pm 0.49$

(b) *Brightness*

Shift Step	0	0.01	0.02	0.03
$\gamma = 0.25$	$9.60 \pm 2.33$	$3.40 \pm 0.49$	$1.80 \pm 0.40$	$1.40 \pm 0.49$
$\gamma = 0.5$	$3.00 \pm 0.89$	$1.80 \pm 0.75$	$1.00 \pm 0.00$	$0.60 \pm 0.49$
$\gamma = 0.75$	$0.40 \pm 0.49$	$0.20 \pm 0.40$	$0.00 \pm 0.00$	$0.00 \pm 0.00$

(c) *Hue*

Shift Step	0	0.2	0.4	0.6
$\gamma = 0.25$	$9.00 \pm 2.28$	$2.80 \pm 0.40$	$1.40 \pm 0.49$	$1.20 \pm 0.40$
$\gamma = 0.5$	$3.00 \pm 0.89$	$0.80 \pm 0.40$	$0.20 \pm 0.40$	$0.40 \pm 0.49$
$\gamma = 0.75$	$0.40 \pm 0.49$	$0.00 \pm 0.00$	$0.00 \pm 0.00$	$0.00 \pm 0.00$

(d) *Saturation*

Table 4:  $\gamma$ -survivability of backdoor attacks under different data distribution shifts. The larger the distribution shift, the faster the backdoor gets forgotten. This result is for CIFAR10.

## 5 Impact of Data Distribution Shift

As discussed in §3.2, we emulate a dynamic data environment by introducing parameterized distribution shifts using image transformations. So far our results assume the default data distribution shift (i.e., rotation by  $2^\circ$ ). Next we examine the impact of different data distribution shifts on backdoor survivability. Our goal is not to compare different transformation types, but to examine how the volume of distribution shifts affects backdoor survivability. Table 4 plots, per transformation type, the backdoor  $\gamma$ -survivability for one-shot poisoning on  $D_1$ , when varying the distribution shift step ( $p$ ). While the value of  $p$  is transformation-specific, larger  $p$  always means heavier data distribution shift over time. We only show the results for CIFAR10 since MNIST displays the same trend.

**Larger data distribution shifts accelerate backdoor forgetting.** Our key observation is that, when the production data experiences heavier changes over time, the backdoors are more vulnerable to model updates. This is because when model updates “force” the time-varying model to learn more different data features, they also accelerate the process of backdoor forgetting. This observation also aligns with recent work on continual learning on old/new (benign) tasks [45], which shows that the larger the distance between two task distributions, the faster the model forgets the old task it has learned previously. Different from [45], we focus on backdoor attacks rather than benign tasks. Overall, our findings further demonstrate the importance of studying backdoor survivability, since data distribution shift is a common phenomenon in practice.

## 6 Smart Training Strategies to Reduce Backdoor Survivability

Our empirical study demonstrates the *backdoor forgetting* property of time-varying DNN models. It also suggests that intelligent training strategies, especially during model fine-tuning, can accelerate backdoor forgetting without compromising normal accuracy. Recall that our baseline strategy for model fine-tuning is stochastic gradient descent (SGD) with a weight decay and momentum factor, using 0.01 learning rate and 5 training epochs.

**Increasing training epochs and learning rate.** We empirically find that both training time (epochs) and learning rate can be better configured to reduce backdoor survivability without harming normal accuracy. These observations are specific to time-varying models and do not apply to static models. More precisely, Table 5a shows that increasing the number of training epochs during model updates from 5 to 10 reduces the backdoor’s 0.25-survivability from 5.4 to 3.6 (for one-shot poisoning on  $D_1$ ). This is likely because additional training epochs allows the model to learn more new data features (and thus forget existing features like the backdoor faster). Similarly, increasing learning rate from 0.01 to 0.1 reduces 0.25-survivability from 5.4 to 1.0 (see Table 5b). Clearly, these values have to be adjusted carefully to weigh the improved forgetfulness of backdoors, against possible downsides such as training overhead and possible overfitting (for more epochs) and lower convergence rates (for larger learning rates).

**Smarter optimizers.** We consider intelligent optimizers that automatically adapt their learning step size. In particular, we repeat the experiments and replace SGD with an Adam optimizer [15]<sup>1</sup>. The resulting backdoor 0.25-survivability is  $3.40 \pm 0.80$ , which lies between 5.4 (SGD with 0.01 learning rate) and 1 (SGD with 0.1 learning rate).

<sup>1</sup>We set the initial learning rate for the Adam optimizer to 0.0001 to optimize normal accuracy.



Training Epochs	5	10	20	Learning Rate	0.005	0.01	0.05	0.1	0.5
$\gamma = 0.25$	$5.40 \pm 0.80$	$3.60 \pm 0.49$	$2.20 \pm 0.40$	$\gamma = 0.25$	$7.20 \pm 0.98$	$5.40 \pm 0.80$	$1.00 \pm 0.63$	$1.00 \pm 0.63$	$0.20 \pm 0.40$
$\gamma = 0.5$	$2.40 \pm 0.49$	$2.00 \pm 0.00$	$1.20 \pm 0.40$	$\gamma = 0.5$	$2.60 \pm 0.49$	$2.40 \pm 0.49$	$0.80 \pm 0.40$	$0.20 \pm 0.40$	$0.00 \pm 0.00$
$\gamma = 0.75$	$0.20 \pm 0.40$	$0.20 \pm 0.40$	$0.00 \pm 0.00$	$\gamma = 0.75$	$0.40 \pm 0.49$	$0.20 \pm 0.40$	$0.00 \pm 0.00$	$0.00 \pm 0.00$	$0.00 \pm 0.00$

(a) Varying # of training epochs per update

(b) Varying learning rate of SGD

Table 5:  $\gamma$ -survivability of one-shot backdoor attacks on  $D_1$  with different training settings.

Metrics	Varying poison ratio					Varying trigger size		
	0.01	0.02	0.05	0.1	0.2	$4 \times 4$	$8 \times 8$	$16 \times 16$
$\gamma = 0.25$	$0.00 \pm 0.00$	$0.00 \pm 0.00$	$0.60 \pm 0.49$	$0.00 \pm 0.00$	$0.00 \pm 0.00$	$0.60 \pm 0.49$	$0.40 \pm 0.49$	$2.00 \pm 1.41$
$\gamma = 0.5$	$0.00 \pm 0.00$	$0.00 \pm 0.00$	$0.00 \pm 0.00$	$0.00 \pm 0.00$	$0.00 \pm 0.00$	$0.00 \pm 0.00$	$0.00 \pm 0.00$	$1.00 \pm 0.63$
$\gamma = 0.75$	$0.00 \pm 0.00$	$0.00 \pm 0.00$	$0.00 \pm 0.00$	$0.00 \pm 0.00$	$0.00 \pm 0.00$	$0.00 \pm 0.00$	$0.00 \pm 0.00$	$0.00 \pm 0.00$

(a) poisoning  $D_1$ 

Metrics	Varying poison ratio					Varying trigger size		
	0.01	0.02	0.05	0.1	0.2	$4 \times 4$	$8 \times 8$	$16 \times 16$
$\gamma = 0.25$	$0.00 \pm 0.00$	$0.00 \pm 0.00$	$0.00 \pm 0.00$	$0.00 \pm 0.00$	$0.00 \pm 0.00$	$0.00 \pm 0.00$	$0.00 \pm 0.00$	$0.20 \pm 0.40$
$\gamma = 0.5$	$0.00 \pm 0.00$	$0.00 \pm 0.00$	$0.00 \pm 0.00$	$0.00 \pm 0.00$	$0.00 \pm 0.00$	$0.00 \pm 0.00$	$0.00 \pm 0.00$	$0.00 \pm 0.00$
$\gamma = 0.75$	$0.00 \pm 0.00$	$0.00 \pm 0.00$	$0.00 \pm 0.00$	$0.00 \pm 0.00$	$0.00 \pm 0.00$	$0.00 \pm 0.00$	$0.00 \pm 0.00$	$0.00 \pm 0.00$

(b) poisoning  $D_0$ Table 6: Backdoor  $\gamma$ -survivability for two types of one-shot poisoning ( $D_0$  and  $D_1$ ), when the time-varying model is updated using STLRs. This result is for CIFAR10.

**Smarter learning rate scheduler (STLR).** We also consider a smarter learning rate scheduler: Slanted Triangular Learning Rates (STLRs) [12]. It first linearly increases the learning rate from 0 to the max value (e.g., up to 0.5) and then linearly decays it back to 0. Interestingly, STLR is highly effective in terms of reducing backdoor survivability.

Table 6 lists the backdoor  $\gamma$ -survivability for one-shot poisoning attacks (on  $D_1$  and  $D_0$ ), when model updates use STLR. The baseline version (e.g., model updates using SGD) is in Table 1. Comparing the two tables, we see that training using STLR naturally removes the backdoor, i.e., an injected backdoor cannot survive past a single model update.

We do note, however, that updating using STLR has limited impact against a persistent poisoning attack, i.e. where the attacker poisons every update’s training data ( $k_p = 1, k_w = 0$ ). This is expected, given the constant influx of additional poison data into each update. Comparing Table 7 to Table 3, we see that STLR’s impact is minimal.

**Summary.** We find that model owners can significantly reduce backdoor survivability by leveraging adaptive learning rate schedulers like STLR, and increasing training epochs. In most cases, all three backdoor survivability metrics drop to 0, meaning the backdoor is immediately removed by a single fine-tuning update. This additional benefit only adds to the existing value of these techniques as ways to enhance model accuracy.

## 7 Conclusion

In this paper, we take a first look at backdoor attacks in the pragmatic context of time-varying models. We introduce the first empirical metric to measure a backdoor’s ability to survive on time-varying models, and study a range of factors that may impact backdoor survivability. For models undergoing periodic fine-tuning, we identify their natural ability to gradually forget backdoor rules generated using one-shot poison attacks. Our study shows that smarter training strategies and well-chosen hyperparameters can further accelerate the degradation of backdoors. These findings significantly increase the difficulty and cost for attackers to perform effective backdoor attacks on time-varying models, and suggest new directions in improving model robustness against poison attacks in time-varying contexts.

As the first study on backdoor survivability, our work faces two key limitations. First, our study focused on two commonly used image datasets to demonstrate the interesting property of “backdoor forgetting.” More empirical and analytical studies are needed to characterize the complex relationship between model updates and backdoor forgetting. Second, we trigger model updates using controlled

Subsequent Poison Ratio	0.0001	0.0002	0.0005	0.001	0.002	0.005
$\gamma = 0.25$	$2.20 \pm 0.98$	$12.80 \pm 1.94$	$14.00 \pm 0.00$	$14.00 \pm 0.00$	$14.00 \pm 0.00$	$14.00 \pm 0.00$
$\gamma = 0.5$	$0.40 \pm 0.49$	$7.80 \pm 4.07$	$14.00 \pm 0.00$	$14.00 \pm 0.00$	$14.00 \pm 0.00$	$14.00 \pm 0.00$
$\gamma = 0.75$	$0.00 \pm 0.00$	$0.80 \pm 1.17$	$10.80 \pm 2.40$	$14.00 \pm 0.00$	$14.00 \pm 0.00$	$14.00 \pm 0.00$

Table 7: Backdoor  $\gamma$ -survivability for persistent poisoning ( $k_p = 1, k_w = 0$ ) when the time-varying model is updated using STLRS. This result is for CIFAR10.

data dynamics via image transformation. Experiments using a broader and more realistic category of data dynamics will provide more insights on how to leverage natural data variations (and thus model variations) to resist backdoor attacks.

## References

- [1] BAGDASARYAN, E., VEIT, A., HUA, Y., ESTRIN, D., AND SHMATIKOV, V. How to backdoor federated learning. In *Proc. of International Conference on Artificial Intelligence and Statistics* (2020), PMLR, pp. 2938–2948.
- [2] BIGGIO, B., NELSON, B., AND LASKOV, P. Poisoning attacks against support vector machines. In *Proc. of ICML* (2012), pp. 1467–1474.
- [3] BLOG, G. C. Mlops: Continuous delivery and automation pipelines in machine learning. <https://cloud.google.com/architecture/mlops-continuous-delivery-and-automation-pipelines-in-machine-learning>.
- [4] CHEN, X., LIU, C., LI, B., LU, K., AND SONG, D. Targeted backdoor attacks on deep learning systems using data poisoning. *arXiv preprint arXiv:1712.05526* (2017).
- [5] DELANGE, M., ALJUNDI, R., MASANA, M., PARISOT, S., JIA, X., LEONARDIS, A., SLABAUGH, G., AND TUYTELAARS, T. A continual learning survey: Defying forgetting in classification tasks. *IEEE Transactions on Pattern Analysis and Machine Intelligence* (2021).
- [6] GAO, Y., DOAN, B. G., ZHANG, Z., MA, S., ZHANG, J., FU, A., NEPAL, S., AND KIM, H. Backdoor attacks and countermeasures on deep learning: A comprehensive review. *arXiv preprint arXiv:2007.10760* (2020).
- [7] GAO, Y., XU, C., WANG, D., CHEN, S., RANASINGHE, D. C., AND NEPAL, S. Strip: A defence against trojan attacks on deep neural networks. In *Proc. of the 35th Annual Computer Security Applications Conference* (2019), pp. 113–125.
- [8] GU, T., DOLAN-GAVITT, B., AND GARG, S. Badnets: Identifying vulnerabilities in the machine learning model supply chain. In *Proc. of Machine Learning and Computer Security Workshop* (2017).
- [9] HE, K., ZHANG, X., REN, S., AND SUN, J. Deep residual learning for image recognition. In *Proc. of CVPR* (2016), pp. 770–778.
- [10] HOI, S. C., SAHOO, D., LU, J., AND ZHAO, P. Online learning: A comprehensive survey. *Neurocomputing* 459 (2021), 249–289.
- [11] HOI, S. C., WANG, J., AND ZHAO, P. Libol: A library for online learning algorithms. *Journal of Machine Learning Research* 15, 1 (2014), 495.
- [12] HOWARD, J., AND RUDER, S. Universal language model fine-tuning for text classification. In *Proc. of the 56th Annual Meeting of the Association for Computational Linguistics (Volume 1: Long Papers)* (2018), pp. 328–339.
- [13] HUANG, G., LIU, Z., VAN DER MAATEN, L., AND WEINBERGER, K. Q. Densely connected convolutional networks. In *Proc. of CVPR* (2017), pp. 4700–4708.
- [14] ILYAS, A., PARK, S. M., ENGSTROM, L., LECLERC, G., AND MADRY, A. Datamodels: Predicting predictions from training data. *arXiv preprint arXiv:2202.00622* (2022).
- [15] KINGMA, D. P., AND BA, J. Adam: A method for stochastic optimization. In *Proc. of ICLR* (2015).
- [16] KRIZHEVSKY, A., ET AL. Learning multiple layers of features from tiny images.
- [17] KUMAR, A., MA, T., AND LIANG, P. Understanding self-training for gradual domain adaptation. In *Proc. of ICML* (2020), PMLR, pp. 5468–5479.
- [18] KUMAR, R. S. S., NYSTRÖM, M., LAMBERT, J., MARSHALL, A., GOERTZEL, M., COMISSONERU, A., SWANN, M., AND XIA, S. Adversarial machine learning-industry perspectives. In *Proc. of 2020 IEEE Security and Privacy Workshops (SPW)* (2020), IEEE, pp. 69–75.
- [19] LECLERC, G., ILYAS, A., ENGSTROM, L., PARK, S. M., SALMAN, H., AND MADRY, A. `ffcv`. <https://github.com/libffcv/ffcv/>, 2022.

- [20] LECUN, Y., BOTTOU, L., BENGIO, Y., AND HAFFNER, P. Gradient-based learning applied to document recognition. *Proc. of IEEE S&P* 86, 11 (1998), 2278–2324.
- [21] LI, Y., LI, Y., WU, B., LI, L., HE, R., AND LYU, S. Invisible backdoor attack with sample-specific triggers. In *Proc. of the IEEE/CVF International Conference on Computer Vision (2021)*, pp. 16463–16472.
- [22] LIN, J., XU, L., LIU, Y., AND ZHANG, X. Composite backdoor attack for deep neural network by mixing existing benign features. In *Proc. of CCS (2020)*, pp. 113–131.
- [23] LIU, K., DOLAN-GAVITT, B., AND GARG, S. Fine-pruning: Defending against backdooring attacks on deep neural networks. In *Proc. of RAID (2018)*.
- [24] LIU, Y., LEE, W.-C., TAO, G., MA, S., AAFER, Y., AND ZHANG, X. Abs: Scanning neural networks for back-doors by artificial brain stimulation. In *Proc. of CCS (2019)*, pp. 1265–1282.
- [25] LIU, Y., MA, S., AAFER, Y., LEE, W.-C., ZHAI, J., WANG, W., AND ZHANG, X. Trojaning attack on neural networks. In *Proc. of NDSS (2018)*.
- [26] NAHAR, N., ZHOU, S., LEWIS, G., AND KÄSTNER, C. Collaboration challenges in building ml-enabled systems: Communication, documentation, engineering, and process. In *Proc. of the 44th International Conference on Software Engineering (ICSE) (5 2022)*.
- [27] NGUYEN, T. A., AND TRAN, A. Input-aware dynamic backdoor attack. *Advances in Neural Information Processing Systems* 33 (2020), 3454–3464.
- [28] PARKHI, O. M., VEDALDI, A., AND ZISSERMAN, A. Deep face recognition.
- [29] QIAO, X., YANG, Y., AND LI, H. Defending neural backdoors via generative distribution modeling. *Advances in neural information processing systems* 32 (2019).
- [30] READ, J., BIFET, A., PFAHRINGER, B., AND HOLMES, G. Batch-incremental versus instance-incremental learning in dynamic and evolving data. In *Proc. of International symposium on intelligent data analysis (2012)*, Springer, pp. 313–323.
- [31] RUSSAKOVSKY, O., DENG, J., SU, H., KRAUSE, J., SATHEESH, S., MA, S., HUANG, Z., KARPATY, A., KHOSLA, A., BERNSTEIN, M., BERG, A. C., AND LI, F.-F. ImageNet Large Scale Visual Recognition Challenge. *International Journal of Computer Vision (IJCV)* 115, 3 (2015), 211–252.
- [32] SAHOO, D., PHAM, Q., LU, J., AND HOI, S. C. Online deep learning: learning deep neural networks on the fly. In *Proc. of the 27th International Joint Conference on Artificial Intelligence (2018)*, pp. 2660–2666.
- [33] STEINHARDT, J., KOH, P. W. W., AND LIANG, P. S. Certified defenses for data poisoning attacks. *Advances in neural information processing systems* 30 (2017).
- [34] TAJBAKSH, N., SHIN, J. Y., GURUDU, S. R., HURST, R. T., KENDALL, C. B., GOTWAY, M. B., AND LIANG, J. Convolutional neural networks for medical image analysis: Full training or fine tuning? *IEEE transactions on medical imaging* 35, 5 (2016), 1299–1312.
- [35] TONEVA, M., SORDONI, A., COMBES, R. T. D., TRISCHLER, A., BENGIO, Y., AND GORDON, G. J. An empirical study of example forgetting during deep neural network learning. In *Proc. of ICLR (2019)*.
- [36] TORREY, L., AND SHAVLIK, J. Transfer learning. In *Handbook of research on machine learning applications and trends: algorithms, methods, and techniques*. IGI global, 2010, pp. 242–264.
- [37] TRAN, B., LI, J., AND MADRY, A. Spectral signatures in backdoor attacks. *Advances in neural information processing systems* 31 (2018).
- [38] VELDANDA, A., AND GARG, S. On evaluating neural network backdoor defenses. *arXiv preprint arXiv:2010.12186* (2020).
- [39] WANG, B., YAO, Y., SHAN, S., LI, H., VISWANATH, B., ZHENG, H., AND ZHAO, B. Y. Neural cleanse: Identifying and mitigating backdoor attacks in neural networks. In *Proc. of IEEE S&P (2019)*, IEEE, pp. 707–723.
- [40] WANG, H., SREENIVASAN, K., RAJPUT, S., VISHWAKARMA, H., AGARWAL, S., SOHN, J.-Y., LEE, K., AND PAPALIOPOULOS, D. Attack of the tails: Yes, you really can backdoor federated learning. *Advances in Neural Information Processing Systems* 33 (2020), 16070–16084.
- [41] WENGER, E., PASSANANTI, J., BHAGOJI, A. N., YAO, Y., ZHENG, H., AND ZHAO, B. Y. Backdoor attacks against deep learning systems in the physical world. In *Proc. of CVPR (2021)*, pp. 6206–6215.
- [42] XIAO, H., XIAO, H., AND ECKERT, C. Adversarial label flips attack on support vector machines. In *Proc. of the 20th European Conference on Artificial Intelligence (2012)*, pp. 870–875.
- [43] XIE, C., HUANG, K., CHEN, P.-Y., AND LI, B. Dba: Distributed backdoor attacks against federated learning. In *Proc. of ICLR (2019)*.
- [44] YAO, Y., LI, H., ZHENG, H., AND ZHAO, B. Y. Latent backdoor attacks on deep neural networks. In *Proc. of CCS (2019)*, pp. 2041–2055.

- [45] YIN, D., FARAJTABAR, M., LI, A., LEVINE, N., AND MOTT, A. Optimization and generalization of regularization-based continual learning: a loss approximation viewpoint. *arXiv preprint arXiv:2006.10974* (2020).
- [46] YOON, J., YANG, E., LEE, J., AND HWANG, S. J. Lifelong learning with dynamically expandable networks. In *Proc. of ICLR* (2018).
- [47] ZHANG, Y., FENG, F., WANG, C., HE, X., WANG, M., LI, Y., AND ZHANG, Y. How to retrain recommender system? a sequential meta-learning method. In *Proc. of the 43rd International ACM SIGIR Conference on Research and Development in Information Retrieval* (2020), pp. 1479–1488.
- [48] ZHUANG, F., QI, Z., DUAN, K., XI, D., ZHU, Y., ZHU, H., XIONG, H., AND HE, Q. A comprehensive survey on transfer learning. *Proc. of IEEE S&P 109*, 1 (2020), 43–76.

## A Details for Experimental Setup

In this section, we provide further information about our experimental setup, expanding upon the background from Section 3.2 of the main paper.

**More details about distribution shifts.** We select 4 types of image transformations, namely: i) rotation, ii) changing brightness, iii) changing hue, and iv) changing saturation. We use these transformations to introduce fine-grained, parameterized data distribution shifts over the sequence of changing data distributions ( $\{D_i\}_{i>0}$ ). When implementing the transformations, we use PyTorch’s built-in functions in `torchvision.transforms.functional` (see Table 8).

Transformation Types	Function Call
Rotation	<code>rotate(<math>X</math>, <math>i \times p</math>)</code>
Brightness	<code>adjust_brightness(<math>X</math>, <math>1 + i \times p</math>)</code>
Hue	<code>adjust_hue(<math>X</math>, <math>i \times p</math>)</code>
Saturation	<code>adjust_saturation(<math>X</math>, <math>1 + i \times p</math>)</code>

Table 8: Function calls for generating training datasets  $D_i$  for different data distribution drifts with given shift steps  $p$ .  $X$  is the original training data with no transformations.

**More details on model training and updating.** To train an initial model  $F_0$ , we choose ResNet-9 as our default model architecture and train the model using  $D_0$  with a batch-size of 512. We train the model for 48 epochs for CIFAR10 and 10 epochs for MNIST. By default, we use an SGD optimizer with momentum= 0.9, weight decay=  $5e - 4$ . When using STLRL, we set the maximum learning rate to 0.9. We also run experiments with two other model architectures (ResNet-18 and DenseNet-121) on CIFAR10. When training an initial model  $F_0$ , we train the model for 80 epochs using the same optimizer settings and the STLRL scheduler as the ResNet-9 experiments.

To update the model (i.e., from  $F_{i-1}$  to  $F_i$ ), our default updating setting is to fine-tune each model  $F_{i-1}$  with the new training data  $D_i$  for 5 epochs using an SGD optimizer with a constant learning rate= 0.01, momentum= 0.9 and weight decay=  $5e - 4$ . We set learning rate= 0.01 since it produces the best normal accuracies among our experiments. In Section 6, we also experiment with an Adam optimizer with learning rate= 0.0001 and weight\_decay=  $5e - 4$ , and an SGD optimizer with STLRL setting max learning rate= 0.5, momentum= 0.9 and weight\_decay=  $5e - 4$ . In these experiments, we examine the experiments carefully to ensure that the normal classification accuracies do not drop compared to those of our default training setting. We show the average normal accuracies and attack success rates as a function of model updates in §B.3.

## B Additional Results

In this section, we provide additional results aside from those listed in the main body of the paper. We start from the key results on backdoor survivability for the MNIST dataset, which produce the same trend as CIFAR10 (see §B.1). We also provide detailed results on the CIFAR10 dataset regarding the impact of trigger size and location on backdoor survivability, as well as those of different model architectures (see §B.2). Finally, we present the normal accuracies for the time-varying models as a function of model updates, for both CIFAR10 and MNIST (see §B.3).

### B.1 Backdoor Survivability Results for MNIST

**One-shot backdoor survivability.** In Table 9, we show the one-shot backdoor survivability result for ResNet-9 trained on MNIST when we vary the poison ratio and trigger size (i.e., reproducing Table 1 from the main paper). These results align with those in Table 1, i.e., (i) backdoors injected by poisoning  $D_0$  (via full training) survive much more updates than those injected by poisoning  $D_1$ ; (ii) trigger size can have a heavy impact on backdoor survivability (especially when poisoning  $D_1$ ); and (iii) increasing poison ratio does not necessarily increase the backdoor survivability.

**Model training using STLRL.** From Table 10, we again see the stark effect of using the STLRL scheduler on backdoor survivability, where the backdoor is unable to survive even a single round of updating in most cases (reproducing Table 6 from the main paper).

Metrics	poison ratio					trigger size		
	0.01	0.02	0.05	0.1	0.2	4 × 4	8 × 8	16 × 16
$\gamma = 0.25$	14.00 ± 0.00	12.80 ± 1.60	14.00 ± 0.00	14.00 ± 0.00	12.80 ± 2.40	14.00 ± 0.00	14.00 ± 0.00	13.40 ± 1.20
$\gamma = 0.5$	13.60 ± 0.80	12.00 ± 2.53	13.80 ± 0.40	14.00 ± 0.00	12.20 ± 3.60	13.80 ± 0.40	13.60 ± 0.80	13.40 ± 1.20
$\gamma = 0.75$	11.60 ± 2.24	11.20 ± 3.49	13.40 ± 1.20	13.40 ± 1.20	11.40 ± 3.88	13.40 ± 1.20	13.20 ± 1.17	13.40 ± 1.20

(a) poisoning  $D_0$ 

Metrics	poison ratio					trigger size		
	0.01	0.02	0.05	0.1	0.2	4 × 4	8 × 8	16 × 16
$\gamma = 0.25$	0.00 ± 0.00	0.60 ± 0.80	1.20 ± 0.75	0.60 ± 0.49	0.20 ± 0.40	1.20 ± 0.75	4.60 ± 3.83	13.60 ± 0.80
$\gamma = 0.5$	0.00 ± 0.00	0.00 ± 0.00	0.40 ± 0.49	0.20 ± 0.40	0.00 ± 0.00	0.40 ± 0.49	2.80 ± 1.33	12.00 ± 1.79
$\gamma = 0.75$	0.00 ± 0.00	0.00 ± 0.00	0.00 ± 0.00	0.00 ± 0.00	0.00 ± 0.00	0.00 ± 0.00	1.40 ± 1.02	8.40 ± 3.26

(b) poisoning  $D_1$ 

Table 9: Backdoor  $\gamma$ -survivability using two types of one-shot poisoning: (a) poisoning  $D_0$  to inject backdoors into  $F_0$  via full training and (b) poisoning  $D_1$  to inject backdoors into  $F_1$  via fine-tuning. This is for MNIST and the model is updated via the default SGD based method.

Metrics	poison ratio					trigger size		
	0.01	0.02	0.05	0.1	0.2	4 × 4	8 × 8	16 × 16
$\gamma = 0.25$	0.00 ± 0.00	0.00 ± 0.00	0.00 ± 0.00	0.00 ± 0.00	0.00 ± 0.00	0.00 ± 0.00	0.00 ± 0.00	2.20 ± 0.75
$\gamma = 0.5$	0.00 ± 0.00	0.00 ± 0.00	0.00 ± 0.00	0.00 ± 0.00	0.00 ± 0.00	0.00 ± 0.00	0.00 ± 0.00	1.00 ± 0.63
$\gamma = 0.75$	0.00 ± 0.00	0.00 ± 0.00	0.00 ± 0.00	0.00 ± 0.00	0.00 ± 0.00	0.00 ± 0.00	0.00 ± 0.00	0.00 ± 0.00

(a) poisoning  $D_0$ 

Metrics	poison ratio					trigger size		
	0.01	0.02	0.05	0.1	0.2	4 × 4	8 × 8	16 × 16
$\gamma = 0.25$	0.00 ± 0.00	0.00 ± 0.00	0.00 ± 0.00	0.00 ± 0.00	0.00 ± 0.00	0.00 ± 0.00	0.00 ± 0.00	4.00 ± 1.10
$\gamma = 0.5$	0.00 ± 0.00	0.00 ± 0.00	0.00 ± 0.00	0.00 ± 0.00	0.00 ± 0.00	0.00 ± 0.00	0.00 ± 0.00	1.20 ± 0.40
$\gamma = 0.75$	0.00 ± 0.00	0.00 ± 0.00	0.00 ± 0.00	0.00 ± 0.00	0.00 ± 0.00	0.00 ± 0.00	0.00 ± 0.00	0.20 ± 0.40

(b) poisoning  $D_1$ 

Table 10: Backdoor  $\gamma$ -survivability for two types of one-shot poisoning ( $D_0$  and  $D_1$ ). This result is for MNIST and the model is updated using the STLR-based method.

## B.2 Additional Results for CIFAR10

**Impact of trigger location on backdoor survivability.** We find that placing the trigger in the middle of the image makes the backdoor more persistent. Specifically, we experiment with placing a  $4 \times 4$  yellow trigger on the top left (tl), top right (tr), bottom left (bl), bottom right (br), top middle (tm), left middle(lm), bottom middle(bm) and in the center (cen) of the input (as shown in Figure 5). The corresponding backdoor survivability results are shown in Table 11a. We see that, in general, putting the backdoor trigger close to the center of the image produces larger survivability values. One possible explanation is that putting the trigger at the key, discriminative regions used by the model to make classification decisions will make it easier to affect model classification results, thus making the backdoor harder to “forget” during model updates.

**Impact of trigger shape on backdoor survivability.** We then try 5 different trigger shapes while maintaining the same size (16 pixels in total) and a similar location: square, vertical rectangle (vrect), horizontal rectangle (hrect), circle and triangle (see Figure 6). The corresponding backdoor

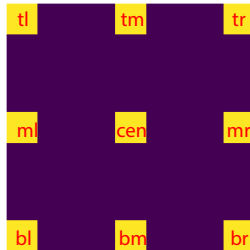


Figure 5: Masks for different trigger locations.

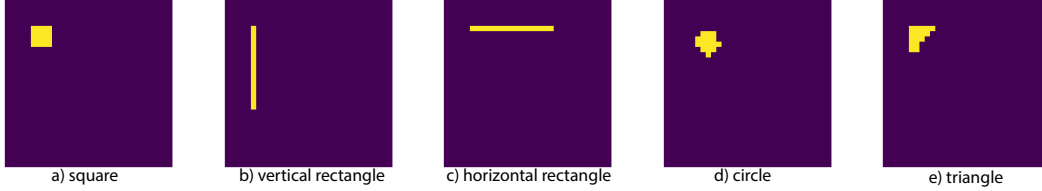


Figure 6: Masks for different trigger shapes.

	top-left	top-right	bottom-left	bottom-right	top-middle	middle-left	middle-right	bottom-middle	center
$\gamma = 0.25$	$2.60 \pm 1.02$	$4.60 \pm 0.80$	$5.00 \pm 1.41$	$9.20 \pm 1.94$	$6.60 \pm 1.02$	$7.60 \pm 1.20$	$7.80 \pm 1.60$	$9.00 \pm 2.00$	<b><math>10.20 \pm 1.72</math></b>
$\gamma = 0.5$	$1.40 \pm 0.49$	$2.40 \pm 0.80$	$2.60 \pm 1.02$	$4.40 \pm 1.62$	$3.20 \pm 0.98$	$3.80 \pm 0.75$	$3.80 \pm 0.98$	$5.20 \pm 1.33$	<b><math>5.40 \pm 1.36</math></b>
$\gamma = 0.75$	$0.80 \pm 0.40$	$1.00 \pm 0.63$	$0.60 \pm 0.49$	$1.00 \pm 0.63$	$1.20 \pm 0.40$	$1.00 \pm 0.63$	$1.00 \pm 0.63$	$1.60 \pm 0.80$	<b><math>2.20 \pm 0.98</math></b>

(a) Varying trigger location

Trigger Shape	square	vrect	hrect	circle	triangle
$\gamma = 0.25$	$5.20 \pm 0.98$	$5.60 \pm 1.02$	$7.80 \pm 1.47$	$6.20 \pm 1.33$	$4.80 \pm 0.40$
$\gamma = 0.5$	$1.80 \pm 0.40$	$2.60 \pm 0.49$	$3.40 \pm 1.36$	$4.20 \pm 1.17$	$2.20 \pm 0.40$
$\gamma = 0.75$	$0.60 \pm 0.49$	$0.60 \pm 0.49$	$0.80 \pm 0.40$	$0.80 \pm 0.40$	$0.20 \pm 0.40$

(b) Varying trigger shape

Table 11: Backdoor  $\gamma$ -survivability with different trigger locations and shapes using one-shot poisoning on  $D_1$ . This is for CIFAR10, and the model is updated via the default SGD method.

survivability results are in Table 11. Among the five tested, ‘hrect’ and ‘circle’ are the best in backdoor survivability, although their advantages are not significant. We also note that it is challenging to conclusively determine which trigger shape is the best since it inevitably interacts with the position of the trigger. Thus compared to trigger size, the impact of trigger shape is much less predictable (and observable).

**Effectiveness of STLRs on different trigger locations and shapes.** We also provide additional results on varying trigger locations and shapes, when STLRs are used for model training/updates. The results in Table 12 complement those of Table 6(a) in the main paper (which varies poison ratio and trigger size). Comparing Table 12 with Table 11, we again observe that the use of STLRs during model updating drastically reduces backdoor survivability across a variety of triggers locations and shapes.

Trigger Location	tl	tr	bl	br	tm	ml	mr	bm	cen
$\alpha = 0.25$	$0.20 \pm 0.40$	$0.00 \pm 0.00$	$0.00 \pm 0.00$	$0.00 \pm 0.00$	$0.00 \pm 0.00$	$0.40 \pm 0.49$	$0.40 \pm 0.49$	$0.20 \pm 0.40$	$1.00 \pm 0.00$
$\alpha = 0.5$	$0.00 \pm 0.00$	$0.00 \pm 0.00$	$0.00 \pm 0.00$	$0.00 \pm 0.00$	$0.00 \pm 0.00$	$0.00 \pm 0.00$	$0.00 \pm 0.00$	$0.00 \pm 0.00$	$0.20 \pm 0.40$
$\alpha = 0.75$	$0.00 \pm 0.00$	$0.00 \pm 0.00$	$0.00 \pm 0.00$	$0.00 \pm 0.00$	$0.00 \pm 0.00$	$0.00 \pm 0.00$	$0.00 \pm 0.00$	$0.00 \pm 0.00$	$0.00 \pm 0.00$

(a) Varying trigger location

Trigger Shape	square	vrect	hrect	circle	triangle
$\alpha = 0.25$	$0.00 \pm 0.00$	$0.60 \pm 0.49$	$0.00 \pm 0.00$	$0.20 \pm 0.40$	$0.00 \pm 0.00$
$\alpha = 0.5$	$0.00 \pm 0.00$	$0.40 \pm 0.49$	$0.00 \pm 0.00$	$0.00 \pm 0.00$	$0.00 \pm 0.00$
$\alpha = 0.75$	$0.00 \pm 0.00$	$0.00 \pm 0.00$	$0.00 \pm 0.00$	$0.00 \pm 0.00$	$0.00 \pm 0.00$

(b) Varying trigger shape

Table 12: Backdoor  $\gamma$ -survivability with different trigger locations and shapes using one-shot poisoning on  $D_1$ . The model is updated using STLRs. This is for CIFAR10.

**Results of ResNet-18 and DenseNet-121.** We also experiment with two other model architectures (ResNet-18 and DenseNet-121). The results in Table 13 (one-shot poisoning of  $D_1$ ) confirm that the backdoor attack success rate consistently decreases over time as the model gets updated. Interestingly, this specific backdoor trigger survives much shorter on ResNet-18 compared to DenseNet-121 (and also ResNet-9). We leave the investigation on the impact of model architecture on specific backdoor survivability to future work.

Another key observation is the model training/updates using STLRs effectively nullifies the successfully injected backdoor using just one model update. This observation aligns with those in the main paper, confirming the benefits of using STLRs in model training.

Poison Ratio	Default model update via SGD					STLR based model update				
	0.01	0.02	0.05	0.1	0.2	0.01	0.02	0.05	0.1	0.2
$\gamma = 0.25$	0.00 $\pm$ 0.00	0.00 $\pm$ 0.00	0.60 $\pm$ 0.49	0.60 $\pm$ 0.49	0.20 $\pm$ 0.40	0.00 $\pm$ 0.00	0.00 $\pm$ 0.00	0.00 $\pm$ 0.00	0.00 $\pm$ 0.00	0.00 $\pm$ 0.00
$\gamma = 0.5$	0.00 $\pm$ 0.00	0.00 $\pm$ 0.00	0.00 $\pm$ 0.00	0.00 $\pm$ 0.00	0.00 $\pm$ 0.00	0.00 $\pm$ 0.00	0.00 $\pm$ 0.00	0.00 $\pm$ 0.00	0.00 $\pm$ 0.00	0.00 $\pm$ 0.00
$\gamma = 0.75$	0.00 $\pm$ 0.00	0.00 $\pm$ 0.00	0.00 $\pm$ 0.00	0.00 $\pm$ 0.00	0.00 $\pm$ 0.00	0.00 $\pm$ 0.00	0.00 $\pm$ 0.00	0.00 $\pm$ 0.00	0.00 $\pm$ 0.00	0.00 $\pm$ 0.00

(a) *ResNet-18*

Poison Ratio	Default model update via SGR					STLR based model update				
	0.01	0.02	0.05	0.1	0.2	0.01	0.02	0.05	0.1	0.2
$\gamma = 0.25$	4.40 $\pm$ 1.36	5.80 $\pm$ 1.47	6.40 $\pm$ 1.02	6.80 $\pm$ 1.47	3.60 $\pm$ 2.58	0.00 $\pm$ 0.00	0.00 $\pm$ 0.00	0.00 $\pm$ 0.00	0.00 $\pm$ 0.00	0.00 $\pm$ 0.00
$\gamma = 0.5$	1.40 $\pm$ 1.02	2.40 $\pm$ 1.20	3.20 $\pm$ 1.47	1.80 $\pm$ 1.94	0.20 $\pm$ 0.40	0.00 $\pm$ 0.00	0.00 $\pm$ 0.00	0.00 $\pm$ 0.00	0.00 $\pm$ 0.00	0.00 $\pm$ 0.00
$\gamma = 0.75$	0.20 $\pm$ 0.40	0.60 $\pm$ 0.80	0.80 $\pm$ 1.17	0.20 $\pm$ 0.40	0.00 $\pm$ 0.00	0.00 $\pm$ 0.00	0.00 $\pm$ 0.00	0.00 $\pm$ 0.00	0.00 $\pm$ 0.00	0.00 $\pm$ 0.00

(b) *DenseNet-121*

Table 13: Backdoor  $\gamma$ -survivability of one-shot poisoning on  $D_1$ , using two other model architectures (ResNet-18 and DenseNet-121). Here we compare the results when the model is trained/updated using the default SGD optimizer, to those using STLRs. We see that model training using STLRs successfully nullifies inject backdoors using just one model update. This result is for CIFAR10.

### B.3 Normal Classification Accuracy of Time-varying Models

We now present the time-varying model’s normal classification accuracy. Since we consider two types of model training/updating methods, i.e., the default SGD based method and the STLR based method, we will present two sets of results, one for each training method.

For both CIFAR10 and MNIST, we train the initial model  $F_0$  to reach a high normal classification accuracy: 92% for CIFAR10 and 98% for MNIST. As we gradually introduce data distribution shifts via image transformations, the model accuracy drops in absence of model updates. For example, after 15 rounds of  $p = 2^\circ$  image rotations, the normal classification accuracy drops from 92% down to 47% for CIFAR10, and from 99% to 91% for MNIST, as shown in Figure 7. When we apply the default SGD based method to update the model via fine-tuning, the normal accuracy remains at 83% and above for CIFAR10 and 98% for MNIST. For other three (less drastic) transformations (i.e., changing brightness, saturations or hue), the time-varying model maintains a 90% normal accuracy for CIFAR10 (Figure 8).

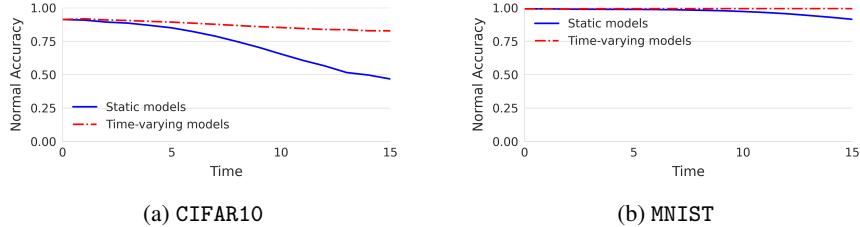


Figure 7: Normal classification accuracy of a static model and a time-varying model (updated via SGD based fine-tuning), when the test data distribution drifts over time. The drift is introduced by rotating the images by  $2^\circ$  each time.

**Normal accuracy using STLR-based updates.** Finally, when using STLR assisted model updates, the normal classification accuracy is nearly identical to that of the default SGD-based method, for both CIFAR10 and MNIST (see Figure 9). This shows that STLR-based model updates can effectively suppress backdoors using just one model update without affecting normal classification accuracy.



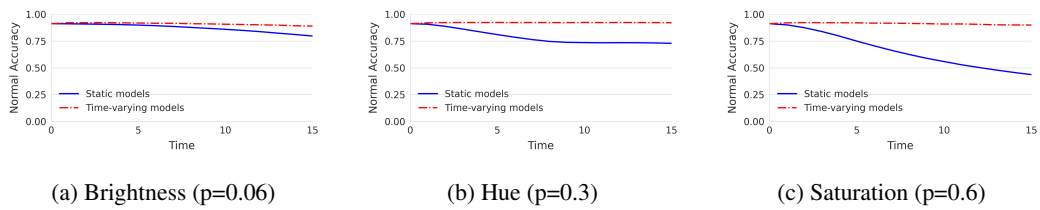


Figure 8: Normal classification accuracy of a static model and a time-varying model (updated via SGD based fine-tuning), when the test data distribution drift is introduced by three other image transformations. This is for CIFAR10.

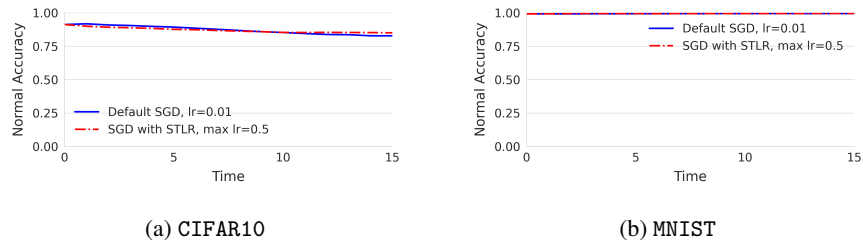


Figure 9: Normal accuracy of time-varying models updated with the default SGD method and the STLR-based method.